International Journal of Pharmaceutics xxx (2011) xxx–xxx

Contents lists available at ScienceDirect

International Journal of Pharmaceutics

journal homepage: www.elsevier.com/locate/ijpharm

Pharmaceutical Nanotechnology

Curcumin and its nano-formulation: The kinetics of tissue distribution and blood–brain barrier penetration

Yin-Meng Tsai [a], Chao-Feng Chien [a], Lie-Chwen Lin [a,b], Tung-Hu Tsai [a,c,*]

[a] Institute of Traditional Medicine, School of Medicine, National Yang-Ming University, Taipei 112, Taiwan
[b] National Research Institute of Chinese Medicine, Taipei, Taiwan
[c] Department of Education and Research, Taipei City Hospital, Taipei, Taiwan

GRAPHICAL ABSTRACT

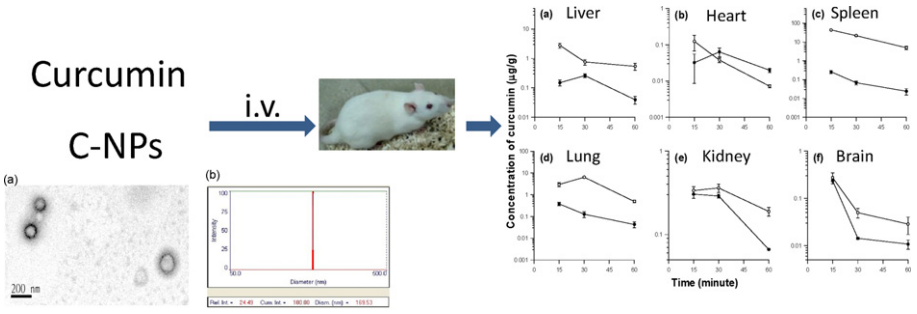

ARTICLE INFO

Article history:
Received 2 March 2011
Received in revised form 7 June 2011
Accepted 17 June 2011
Available online xxx

Keywords:
Curcumin
PLGA
Nanoparticles
Blood–brain barrier
Pharmacokinetics

ABSTRACT

Curcumin has considerable neuro-protective and anti-cancer properties but is rapidly eliminated from the body. By optimizing the HPLC method for analysis of curcumin, this study evaluates how the ability of curcumin to penetrate organs and different regions of the brain is affected by nanoparticulation to increase curcumin circulation time in the body. Curcumin-loaded PLGA nanoparticles (C-NPs) were prepared by the high-pressure emulsification-solvent evaporation method. The mean particle size and entrapment efficiency were 163 nm and 46.9%, respectively. The release profile of C-NPs was an initial burst effect followed by sustained diffusion. In distribution studies, curcumin could be detected in the evaluated organs, including liver, heart, spleen, lung, kidney and brain. C-NPs were found mainly in the spleen, followed by the lung. Formulation significantly raised the curcumin concentration in these organs with increases in the AUC, $t_{1/2}$ and MRT of curcumin, though this was not apparent in the heart. Curcumin and C-NPs could cross the blood–brain barrier (BBB) to enter brain tissue, where it was concentrated chiefly in the hippocampus. Nanoparticulation significantly prolonged retention time of curcumin in the cerebral cortex (increased by 96%) and hippocampus (increased by 83%). These findings provide further understanding for the possible therapeutic effects of curcumin and C-NPs in further pre-clinical and clinical research.

1. Introduction

Curcumin is a polyphenol extracted from the herb *Curcuma longa* L. It has the chemical structure (1,7-bis (4-hydroxy-3-methoxyphenyl)-1,6-heptadiene-3,5-dione) and is water-insoluble. Curcumin is widely used in traditional Chinese medicine and in the food industry (Ammon and Wahl, 1991). It

* Corresponding author at: National Yang-Ming University, School of Medicine, Institute of Traditional Medicine, Taipei 112, Taiwan. Tel.: +886 2 2826 7115; fax: +886 2 2822 5044.
E-mail address: thtsai@ym.edu.tw (T.-H. Tsai).

0378-5173/$ – see front matter © 2011 Elsevier B.V. All rights reserved.
doi:10.1016/j.ijpharm.2011.06.030

also has demonstrated several types of biological and pharmacological activities, including anticancer, anti-inflammatory and antioxidant properties (Shehzad et al., 2010). In addition, curcumin has been shown to have the possibility of slowing the progress of Alzheimer's disease by reducing amyloid β (Garcia-Alloza et al., 2007), of delaying the onset of kainic acid-induced seizures (Sumanont et al., 2007) and of inhibiting the formation of brain tumors (Purkayastha et al., 2009). However, previous studies have shown that the retention time of curcumin in body is limited due to its rapid systemic elimination (Yang et al., 2007). Therefore, the therapeutic efficacy of curcumin is restricted due to its short systemic retention in circulation.

To increase the retention time of curcumin in the body, various formulation techniques have been applied. For example, curcumin–phospholipid complex can extend the retention of curcumin in rat serum (Mythri et al., 2007). Another study has shown that the MRT of curcumin is significantly raised after micellar formulation (Ma et al., 2007). Recently, Mohanty and Sahoo (2010) found that the half-life of curcumin is increased when encapsulated with glycerol monooleate. Furthermore, Anand et al. (2007) have demonstrated that polyester nanoparticle-based delivery systems are favorable for hydrophobic compounds and enhance the bioavailability of poorly water-soluble agents. Polyesters such as poly(lactic-*co*-glycolic acid) (PLGA) are the material generally used for nano-formulation since they are biodegradable, biocompatible, have versatile degradation kinetics (Park, 1995) and have been approved by the U.S. Food and Drug Administration for pharmaceutical application. Therefore, recent in vitro studies have revealed that curcumin inhibition of cancer cell growth was effected by curcumin-loaded PLGA nanoparticles due to enhanced uptake by cells (Anand et al., 2010). The therapeutic effects of curcumin on metastatic cancer cells are also increased after encapsulation with PLGA nanoparticles (Yallapu et al., 2010).

Even though curcumin-loaded PLGA nanoparticles (C-NPs) are effective against cancer (Anand et al., 2010; Yallapu et al., 2010), there have been few studies investigating the organ distribution of curcumin and C-NPs. This is a significant area of research since the organ distribution is a crucial factor for a drug to exhibit therapeutic effects in a target site. Thus, the application of curcumin and effects of its formulation could be clarified by obtaining information on its distribution in the body. The present work evaluates the ability of curcumin and C-NPs to be distributed to brain regions and other organs, together with the pharmacokinetic parameters of curcumin and C-NPs in those areas of the body.

2. Materials and methods

2.1. Materials

Poly(vinyl alcohol) (PVA, M_w: 9000–10,000), PLGA (50:50, M_w: 5000–15,000), sucrose, monosodium phosphate (NaH_2PO_4), polyethylene glycol (PEG) 400, 2-(4′-hydroxybenzeneazo) benzoic acid (as internal standard, IS, of HPLC analysis) and heparin were purchased from Sigma-Aldirch (St. Louis, MO, USA). Curcumin (purity ≥ 95%) was obtained from Fluka (Buchs, Switzerland). Dichloromethane and acetonitrile were purchased from Merck (Darmstadt, Germany). Milli-Q grade water (Millipore, Bedford, MA, USA) was used for the preparation of solution and mobile phase.

2.2. Curcumin nanoparticles procedures

PLGA nanoparticles encapsulating curcumin were prepared by the high-pressure emulsification-solvent evaporation technique (Tsai et al., 2011). Briefly, 50 mg of PLGA and 5 mg of curcumin were dissolved in 1.25 ml dichloromethane as an oil phase. This oil phase was added to 10 ml of aqueous phase (consisted of 2%, PVA and 20%, sucrose, w/v) and then homogenized by homogenizer (Polytron PT-MR 2100, Kinematica AG, Lucerne, Switzerland) at 28,000 rpm for 10 min to form an emulsion. This emulsion was passed through a 0.1 μm filter twice at an operating pressure of 5 kg/cm^2 by extruder accessory (EF-C5, Avestin, Canada) to formulate the C-NPs. The resulting nanoparticles were kept overnight with stirring at 500 rpm to evaporate the organic solvent by air drying (Jaiswal et al., 2004), thus yielding the finial C-NP solution.

2.3. Nanoparticle characteristics

2.3.1. Particle size, polydispersity index and zeta potential

The particle size and polydispersity index (PDI) of C-NPs were measured by dynamic light scattering (90Plus, BIC, Holtsville, NY, USA). The zeta potential of C-NPs was determined using a Zeta potential analyzer (90Plus, BIC).

2.3.2. Entrapment efficiency

Entrapment efficiency estimated the amount of curcumin encapsulated in PLGA nanoparticles. The C-NP solution was centrifuged at 11,000 rpm for 15 min (Centrifuge 5415R, Eppendorf, Germany). After centrifugation, the supernatant was removed and 1 ml of acetonitrile was added to the nanoparticle pellets and then treated with sonication for 5 min to break the nanoparticle structure and release curcumin. The amount of curcumin in nanoparticles was analyzed by HPLC system, as described in Section 2.4. The % entrapment efficiency was given by: $[(\text{Curcumin}_{\text{encapsulated}}/\text{Curcumin}_{\text{total}}) \times 100]$ (Tsai et al., 2011).

2.3.3. Transmission electron microscopy (TEM)

The procedure for TEM samples followed Liang et al. (2005). In brief, the C-NP solution was placed dropwise onto a 400 mesh copper grid coated with carbon. About 15 min after nanoparticle deposition, the grid was tapped with filter paper to remove excess water and stained using a solution of phosphotungsten acid (2%, w/v) for 20 min. After the stained sample was allowed to air dry, TEM samples were obtained. A photomicrogram of C-NPs was obtained by using a transmission electron microscope (JEM-2000EXII, JEOL, Tokyo, Japan).

2.3.4. In vitro drug release study

Release of curcumin from the PLGA nanoparticles was performed by the dialysis membrane method (Shaikh et al., 2009). First, 1 ml of C-NPs solution (equivalent to 0.25 mg of curcumin) was transferred in dialysis bags (Sigma, St. Louis, MO, USA) with a molecular cut-off 3.5 kDa. The bags were suspended in 200 ml of 0.9% normal saline (contain 50%, v/v, of ethanol) at 37 °C in a shaking water bath at 100 rpm (Shaikh et al., 2009). At selected time intervals, 200 μl of normal saline sample was collected and replaced by an equal volume of fresh medium. The curcumin content of normal saline was analyzed by an HPLC system.

2.3.5. Condensation of C-NPs

Since the volume of intravenous administration for a rat is limited, we employed high-speed centrifugation and re-suspension to concentrate the C-NPs. The effect of condensation on nanoparticle characteristics was also investigated by centrifuging 10 ml of C-NPs solution at 11,000 rpm for 15 min. After centrifugation and removing the supernatant, the C-NP pellet was re-suspended in 0.4 ml of an aqueous phase mixture composed of A solution (1% PVA and 10% sucrose, w/v) and B solution (20% PEG 400 and 10% ethanol, v/v) at a ratio of 1:1. The particle sizes, zeta potential, PDI and entrapment efficiency of C-NPs after condensation were determined as

Please cite this article in press as: Tsai, Y.-M., et al., Curcumin and its nano-formulation: The kinetics of tissue distribution and blood–brain barrier penetration. Int J Pharmaceut (2011), doi:10.1016/j.ijpharm.2011.06.030

described above. Final concentration of curcumin in C-NPs after nanoparticle condensation was confirmed by the HPLC system.

2.4. HPLC system and analytical method validation

2.4.1. HPLC system

The HPLC system consisted of a chromatographic pump (LC-20AT, Shimadzu, Kyoto, Japan), autosampler (SIL-20AT, Shimadzu), diode array detector (SPD-M20A, Shimadzu), and degasser (DG-240). For HPLC separation, a reversed-phase C18 column (4.6 × 150 mm, particle size 5 μm, Eclipse XDB, Agilent, Palo Alto, CA, USA) was used. The mobile phase was composed of acetonitrile-10 mM monosodium phosphate (pH 3.5 adjusted by orthophosphoric acid) (40:60, v/v) at a flow-rate of 0.8 ml/min. The run time for analysis was 27 min and the detection wavelength was set at 425 nm. The mobile phase was filtered through a 0.45 μm Millipore membrane filter and degassed by sonication 2510R-DTH (Bransonic, CT, USA) before use. The sample injection volume was 20 μl.

2.4.2. Analytical method validation

The stock solution of curcumin in acetonitrile (500 μg/ml) was diluted with 50% acetonitrile to make serial concentrations of the working standard solutions (0.1, 0.25, 1, 2.5, 10 and 25 μg/ml). Calibration standards were prepared by 5 μl of the working standard solution spiked with 45 μl of blank plasma and organ tissue (liver, heart, spleen, lung, kidney, brain). Extraction procedures followed the sample preparation as described in Section 2.6. The calibration curves were given by: (curcumin peak area/IS peak area for *y*-axis and curcumin concentration for *x*-axis). The limit of detection (LOD) and the limit of quantification (LOQ) were defined as a signal-to-noise ratio of 3 and the lowest concentration of the linear regression, respectively. The accuracy and precision of intra-day (on the same day) and inter-day (on six sequential days) for the curcumin were assayed (six individual tests). The accuracy (% bias) was calculated as $[(C_{obs}-C_{nom})/C_{nom}] \times 100$, where C_{nom} represented the nominal concentration and C_{obs} indicated the mean value of the observed concentration. Precision as the relative standard deviation (RSD) was calculated from the observed concentrations as follows: % RSD = [standard deviation (SD)/C_{obs}] × 100. The % bias and % RSD value for the lowest acceptable reproducibility concentrations was defined as being within ±15%. The recoveries (%) were calculated by comparing the curcumin peak area of the extracted sample with that of the unextracted curcumin standard solution containing the equivalent amount of curcumin in three replicates (at concentrations of 0.1, 0.25 and 2.5 μg/ml).

2.5. Animal study

Male Sprague-Dawley rats (210 ± 10 g body weight) were obtained from the Laboratory Animal Center at National Yang-Ming University (Taipei, Taiwan). These animals were specifically pathogen-free and were allowed to adapt to their environmentally controlled quarters (24 ± 1 °C and 12:12 h light–dark cycle). Food (Laboratory Rodent Diet No. 5001, PMI Feeds Inc., Richmond, IN, USA) and water were available *ad libitum*. All animal experiments were performed according to the National Yang-Ming University guidelines, principles, and procedures for the care and use of laboratory animals.

Experimental rats were initially anesthetized by a mixture (1 ml/kg, i.p.) of urethane (1 g/ml) and α-chloralose (0.1 g/ml). The femoral vein was catheterized with polyethylene tubing for i.v. administration under anesthesia. Then 25 mg/kg of curcumin and of C-NPs, each dissolved in an aqueous phase mixture as described in Section 2.3.5, was intravenously injected via the femoral vein tubing. A 500 μl blood sample was obtained by cardiac puncture with a heparinized syringe and the SD rat was then perfused with normal saline at 15, 30 and 60 min after curcumin and C-NPs administration. The organs (liver, heart, spleen, lung, kidney and brain) were removed and transferred into 50 ml tubes. The brain stem, cerebellum, cerebral cortex, hippocampus, striatum and other parts of the brain were also dissected.

2.6. Sample preparation

The blood sample was centrifuged at 6000 rpm for 10 min at 4 °C for plasma preparation. The supernatant was collected as plasma samples, and preserved at −20 °C before further sample analysis.

The organs and regions of the brain were weighed and homogenized with 50% aqueous acetonitrile (1:5, w/v). The organs and brain tissue samples were then centrifuged at 6000 rpm for 10 min at 4 °C and the supernatant was collected and preserved at −20 °C before further sample assay.

Each biological sample (50 μl) was vortex-mixed with 100 μl of IS solution [containing 1.5 μg/ml of 2-(4′-hydroxybenzeneazo) benzoic acid dissolved in acetonitrile] for protein precipitation. After centrifuging at 12,000 rpm for 15 min, 20 μl of supernatants were collected and analyzed by the HPLC system.

2.7. Pharmacokinetic application and statistics

Pharmacokinetic calculations were performed on each individual set of data using the WinNonlin Standard Edition Version 1.1 (Pharsight Corp., Mountain View, CA, USA) by non-compartmental method. Pharmacokinetic results are represented as mean ± SEM. Statistical analysis was performed by *t* test (SPSS version 10.0 SPSS, Chicago, IL) to compare different groups. The level of significance was set at $p < 0.05$.

3. Results and discussion

3.1. Curcumin-encapsulation in PLGA nanoparticles

Our C-NPs were prepared by the high-pressure emulsification-solvent evaporation technique as in our pervious study (Tsai et al., 2011). For this nano-formulation procedure, PVA was selected as the stabilizer for formulation because it has low toxicity (DeMerlis and Schoneker, 2003). In addition, sucrose was used to increase viscosity of the aqueous phase by decreasing the particle size and PDI of C-NPs (Tsai et al., 2011). In a drug delivery system, particle size greatly influences the pharmacokinetics, including the time of circulation, absorption and distribution (Lankveld et al., 2010). PDI is the index of size distribution that represents the similarity between particles and a large PDI value indicates that the particle sizes are substantially different. Unequal particle size can cause the pharmacokinetic parameters to be irregular and can affect the therapeutic efficiency of a drug-formulation (Müller, 1991).

The properties of nanoparticles after curcumin nano-formulation are shown in Table 1. The size, PDI, zeta potential and encapsulation efficiency of C-NPs were 163 ± 8.1 nm, 0.053 ± 0.021, −12.5 ± 2.8 mV and 46.9 ± 8.2%, respectively. The average diameter distribution (Fig. 1b) and PDI result demonstrated a narrow size distribution of C-NPs. These results indicate that the size of C-NPs is consistent with low PDI. The morphology of C-NPs recorded from TEM was either spherical or ellipsoidal (Fig. 1a) and the particle size (below 200 nm) was similar to the data determined by dynamic light scattering. A recent study demonstrates that nanoparticles smaller than 200 nm are distributed in tumors more efficiently than larger ones (He et al., 2010). The particle size of C-NPs in this article exhibited positive effect on pharmacokinetics, as discussed in Section 3.5.

Please cite this article in press as: Tsai, Y.-M., et al., Curcumin and its nano-formulation: The kinetics of tissue distribution and blood–brain barrier penetration. Int J Pharmaceut (2011), doi:10.1016/j.ijpharm.2011.06.030

Table 1
Properties of C-NPs before and after condensation (mean ± SD, $n = 3$).

Groups	Particle size (nm)	Polydispersity index	Zeta potential (mV)	Encapsulation efficiency (%)
Original	163 ± 8.1	0.053 ± 0.021	−12.5 ± 2.8	46.9 ± 8.2
Condensation	168 ± 9.0	0.085 ± 0.011	−14.1 ± 1.9	44.8 ± 3.6

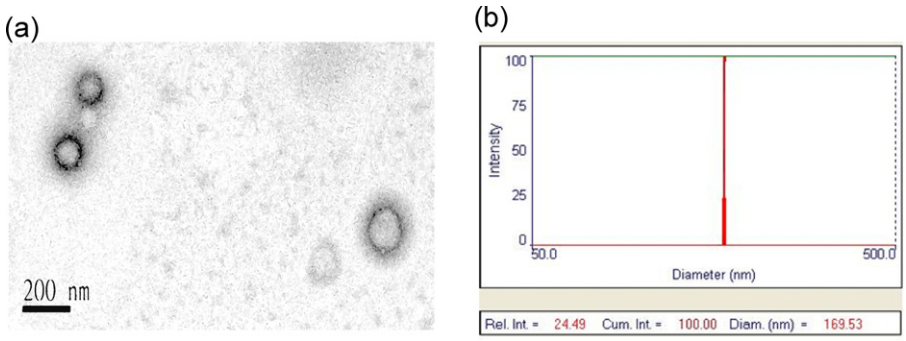

Fig. 1. (a) Morphology by transmission electron microscopy and (b) average size distribution of C-NPs.

3.2. In vitro drug release study

In the formulation system design, it is important that a drug can be readily released from its encapsulating materials such as PLGA because restricted release of a drug from its formulation materials will interfere with the drug availability and reduce the drug efficacy (Müller, 1991). Consequently, to know the in vitro drug release is crucial for drug delivery, the in vitro release profiles of curcumin from PLGA nanoparticles are presented in Fig. 2, which shows a typical biphasic pattern. Initially, a burst release occurred in the first 12 h with 59.0 ± 6.7% of the curcumin released from the PLGA nanoparticles. Following this, a gradual drug release was sustained, with from 59.0 ± 6.7% to 89.7 ± 1.4% of C-NPs released after 6 days. The sustained release profile of curcumin from nanoparticles was consistent with a Higuchi diffusion equation ($r^2 = 0.95$) (Higuchi, 1963). This biphasic release behavior of curcumin from PLGA nanoparticles is consistent with previous research (Shaikh et al., 2009).

Drug release from PLGA microspheres displays multiple release phases, including initial burst release, lag phase and zero order release (Zolnik and Burgess, 2007). The initial burst release is regulated by diffusion of the surface- and pore-associated drug; the lag phase and zero order release are controlled by polymer erosion combined with diffusion (Faisant et al., 2002). Furthermore, Zolnik et al. (2006) demonstrated that low molecular weight of PLGA nanoparticles exhibited diffusion-controlled release. Accordingly, the sustained release of curcumin from nanoparticles prepared with low molecular weight PLGA is controlled by diffusion. Sustained release of the drug in a delivery system is an important property closely related with therapeutic pharmacokinetics and efficacy.

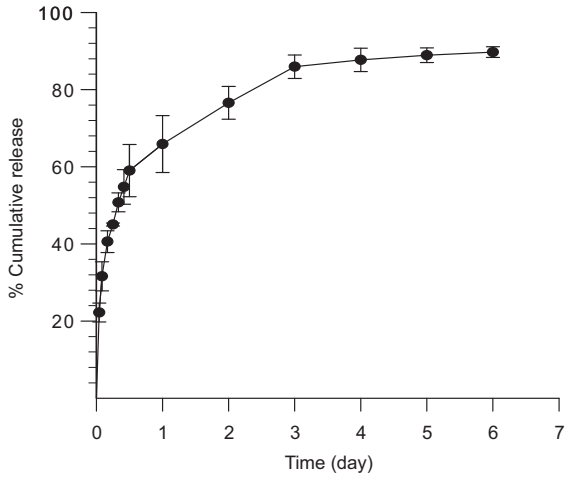

Fig. 2. In vitro release of C-NPs (mean ± SD, $n = 3$).

3.3. Influence of condensation on nanoparticle characteristics

The influence of condensation on particle size, PDI, zeta potential and entrapment efficiency is shown in Table 1. None of the particle characteristics were significantly changed after nanoparticles condensation compared with the original group. Accordingly, this condensation procedure will be applied to concentrate the C-NPs for future animal distribution study. After measurement by HPLC system, the final concentration of C-NPs was 6.4 ± 0.3 mg/ml after particle condensation. A recent study implies that the size of PLGA nanoparticles is significantly increased after freeze-drying, which occurs when using a cryoprotective agent (Shaikh et al., 2009), due to mechanical stress from freeze-drying (Abdelwahed et al., 2006). Therefore, high-speed centrifugation of the nanoparticles followed by re-suspension in an aqueous mixture phase was used to condense the nanoparticles.

3.4. HPLC system and analytic method validation

Fig. 3(a)–(g) shows the chromatograms of blank liver, heart, spleen, lung, kidney, brain and plasma, respectively. Fig. 3(h)–(n) shows chromatograms of the different organ and plasma samples containing the IS and curcumin collected from rats after i.v. administration of C-NPs (25 mg/kg). The retention times of the IS and the curcumin in chromatograms were 6.5 and 22 min, respectively. There were no obvious interference peaks located at the retention times of analyses in the blank chromatograms. These results indicate that the Eclipse XDB-C18 column with the mobile phase of acetonitrile–10 mM monosodium phosphate buffer (pH 3.5) (40:60, v/v) provided good separation and selectivity for curcumin in each biological matrix with these analytical conditions.

The calibration curve for each organ and for plasma had good linearity ($r^2 > 0.995$) over the ranges of 0.025–2.5 μg/ml for organs and 0.01–2.5 μg/ml for plasma, indicating good reproducibility (Chien et al., 2010). The LOD values for curcumin were determined to be

Please cite this article in press as: Tsai, Y.-M., et al., Curcumin and its nano-formulation: The kinetics of tissue distribution and blood–brain barrier penetration. Int J Pharmaceut (2011), doi:10.1016/j.ijpharm.2011.06.030

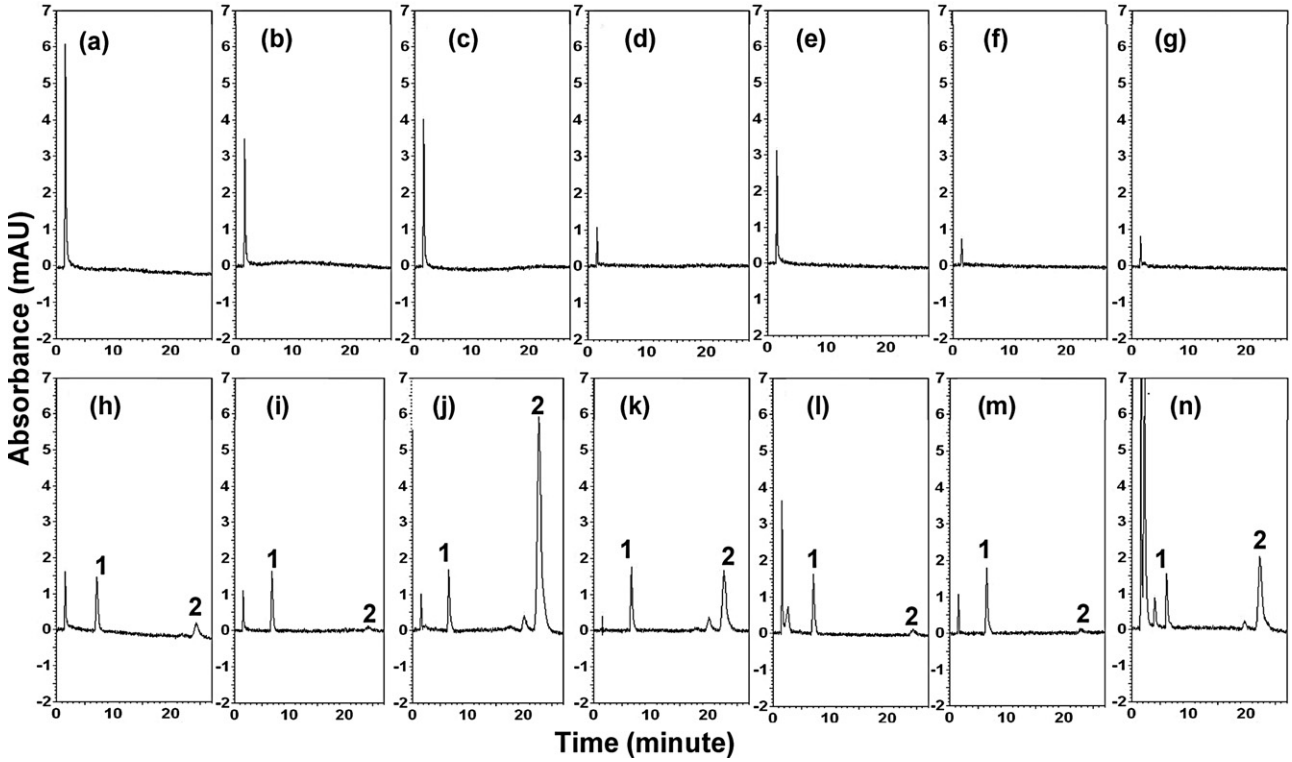

Fig. 3. HPLC chromatograms of (a) blank liver, (b) blank heart, (c) blank spleen, (d) blank lung, (e) blank kidney, (f) blank brain, (g) blank plasma, (h) liver, (i) heart, (j) spleen, (k) lung, (l) kidney, (m) hippocampus, (n) plasma sample collected at 30 min after C-NPs administration (25 mg/kg, i.v.). Peak 1: 2-(4′-hydroxybenzeneazo) benzoic acid, peak 2: curcumin.

0.01 and 0.005 μg/ml for organs and plasma, respectively. The LOQ, defined as the lowest concentration of the linear regression, was 0.025 μg/ml for organs and 0.01 μg/ml for plasma. Intra- and inter-assay accuracy and precision values for curcumin in organs and plasma were all within 15%. These method validation results show that the analytical method for curcumin was optimized for the following pharmacokinetic analysis. The recoveries of curcumin in each of the organs and plasma were higher than 95%, indicating that the efficacy of protein precipitation with acetonitrile at 2-fold volume was sufficient for the separation of the curcumin in those matrices.

3.5. Distribution and pharmacokinetic parameters of curcumin and C-NPs in organs

The concentration–time curves and the pharmacokinetic parameters of curcumin and C-NPs in rat organs are illustrated in Fig. 4 and Table 2, respectively. In the curcumin group, the AUCs of curcumin in liver (9.06 ± 1.55 min μg/ml) and kidney (12.0 ± 0.88 min μg/ml) were larger than in other organs, indicating that more curcumin was in these two organs. One possible reason for these results is that the systemic circulation of curcumin in the body is limited since a substantial amount of curcumin is distributed to the liver and kidney, where it is metabolized and eliminated (Schmidt et al., 2010). However, when C-NPs were intravenously administrated, a significant amount of curcumin was found in the spleen and lung, and the AUC values of curcumin in these organs were 1213 ± 102 min μg/ml and 196 ± 23.1 min μg/ml, respectively (Table 2). The levels of C-NPs amassed in spleen tissue are closely related to phagocytic cell uptake in the reticuloendothelial system (Moghimi et al., 2001). The lung accumulation contributes to the filtration of pulmonary capillary beds following intravenous injection of C-NPs (Mastrobattista et al., 1999). Based on the finding that the main organs of distribution in the C-NPs-treated group, are the spleen and lungs instead of the liver and kidney in conventional curcumin-treated group, the action of nanoparticles in our study is credited with the fact that this formulation prevented curcumin distribution to the major organs metabolizing drugs. Kim et al. (2011) reported that when water-soluble albumin bound-curcumin forms nanoparticles, there is a great quantity of curcumin in the liver, much higher than that in the spleen. This result together with our findings implies that the materials of formulation influence the cell uptake of tissue via changing zeta potential and particle size (Lankveld et al., 2010).

Fig. 4 shows that in rat organs the curcumin levels were increased by nano-formulation, though this did not occur in heart tissue. The low level of C-NPs in the heart was because they were more rapidly eliminated from this organ ($t_{1/2}$ was decreased to 2.8-fold) than the curcumin group. This rapid elimination from the

Table 2
Pharmacokinetic parameters of curcumin and C-NPs in rat organs following i.v. administration.

Organs		$t_{1/2}$ (min)	AUC (min μg/ml)	MRT (min)
Liver	C	17.6 ± 2.20	9.06 ± 1.55	33.0 ± 1.94
	C-NPs	19.8 ± 1.50	71.3 ± 11.7*	35.4 ± 2.40
Heart	C	37.5 ± 9.31	3.03 ± 0.85	57.0 ± 11.1
	C-NPs	13.4 ± 1.81*	2.82 ± 1.14	27.1 ± 2.80*
Spleen	C	12.6 ± 2.46	5.72 ± 1.14	25.6 ± 2.65
	C-NPs	14.2 ± 0.96	1213 ± 102*	28.1 ± 1.18
Lung	C	13.2 ± 1.16	8.98 ± 1.82	26.1 ± 1.11
	C-NPs	15.1 ± 0.48	196 ± 23.1*	30.6 ± 0.36*
Kidney	C	19.7 ± 1.13	12.0 ± 0.88	35.4 ± 1.38
	C-NPs	48.8 ± 0.81*	16.0 ± 1.78	75.7 ± 1.22*
Brain	C	9.20 ± 1.84	4.04 ± 0.22	20.4 ± 0.95
	C-NPs	14.8 ± 1.31*	5.68 ± 1.44	27.1 ± 2.04*

$t_{1/2}$: half-life; AUC: area under the concentration–time curve; MRT: mean residence time; C: curcumin; C-NPs: curcumin nanoparticles (mean ± SEM, $n = 4$).
* $p < 0.05$, vs. curcumin.

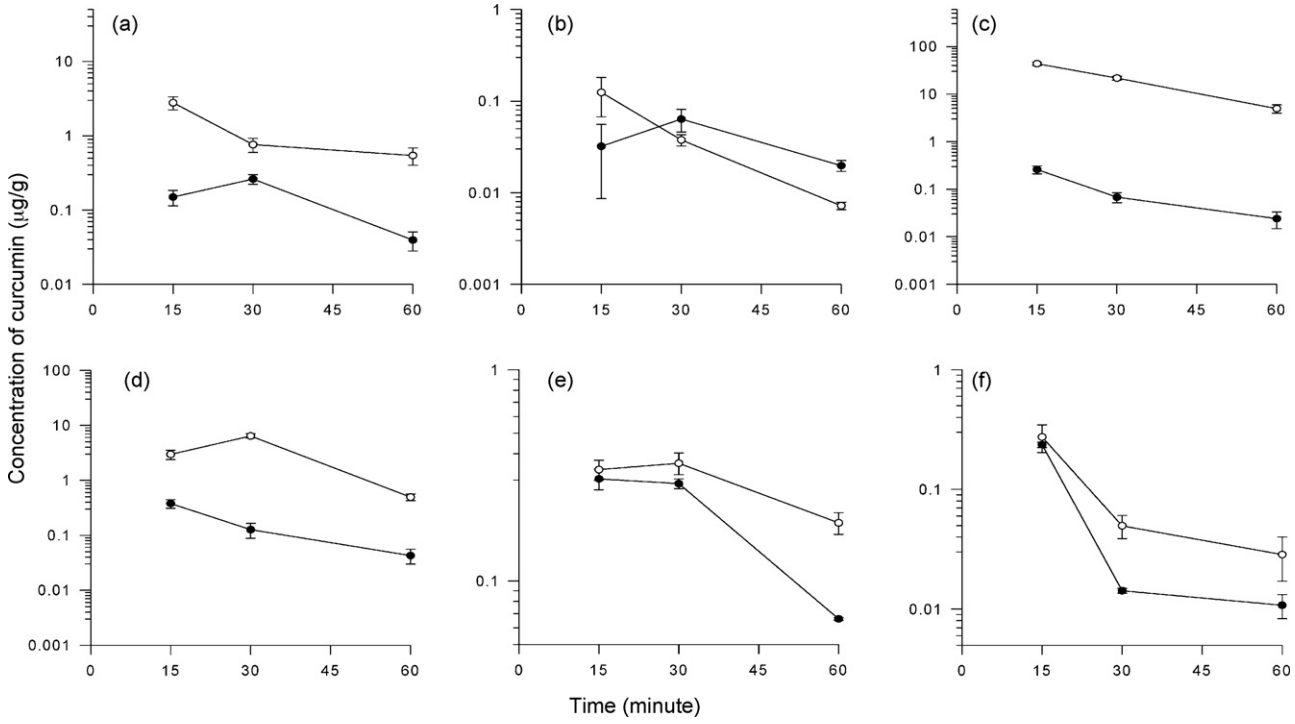

Fig. 4. Concentration–time curve of curcumin and C-NPs in rat (a) liver, (b) heart, (c) spleen, (d) lung, (e) kidney and (f) brain after i.v. administration of curcumin and C-NPs 25 mg/kg (mean ± SEM, $n = 4$). ●: curcumin; ○: C-NPs.

heart may be due to the particle size, which affects the accumulation of nanoparticles in heart cells (Lankveld et al., 2010). This result indicates that C-NPs were less effective on the heart than other organs. Previous studies have reported that curcumin provides immune regulation via spleen tyrosine kinase (Gururajan et al., 2007), protection against lung cancer (Moghaddam et al., 2009), and support of the liver (Wu et al., 2010) and the kidneys (Manikandan et al., 2010). To establish the pharmacodynamic efficacy of a compound, relating the site to the action is required. Results from this study provide solid evidence that curcumin could be detected in the spleen, lung, liver and kidney, where it may be bioactive. Nano-formulation could significantly increase the curcumin levels in these organs because of the increased $t_{1/2}$, AUC and MRT of curcumin (Fig. 4 and Table 2). This suggests that C-NPs may be more efficiently distributed to organs than curcumin alone, thereby supporting therapeutic bioactive properties in the body.

3.6. Distribution and pharmacokinetic parameters of curcumin and C-NPs in regions of the brain

In recent work, curcumin has displayed a substantial neuroprotection ability due to its antioxidant characteristic (Sethi et al., 2009). Fig. 4f clearly shows that curcumin and C-NPs can pass through the BBB into brain tissue. The BBB is a tightly protective reticulum surrounding the brain to restrict substances in the blood from entering the brain. This protective shield is formed at the tight junctions of capillary endothelial cells that contribute to the semi-permeable and selective properties of the BBB. Only drugs with low molecular weight and high lipid solubility of small molecules can cross this specialized system into the brain (Alam et al., 2010). Curcumin is water-insoluble and the formulation material, PLGA, is composed of poly(lactic-*co*-glycolic acid), which has high lipid solubility (Park, 1995). Consequently, the ability of curcumin and its PLGA formulation to cross the BBB into brain regions are closely correlated with its hydrophobic property. After intravenous administration of C-NPs, the MRT of curcumin in the brain was significantly increased (from 20.4 to 27.1) over conventional curcumin, which might be because $t_{1/2}$ was increased significantly (from 9.20 to 14.8) (Table 2). The increased MRT of curcumin in the brain implies that the nanoparticulated formulation prolonged the retention time of curcumin in brain tissue. This prolonged retention time of curcumin in the brain may be because curcumin had sustained diffusion release from biodegradable PLGA nanoparticles (Fig. 2), thereby maintaining curcumin levels in brain tissue.

Fig. 5a shows that 15 min after intravenous injection of C-NPs, the concentration of curcumin in different brain regions was not significantly different from conventional curcumin. However, at 30 min curcumin in the hippocampus was significantly increased with nanoparticulation (Fig. 5b). In addition, although in the other brain regions there was no significant difference between these two groups, curcumin tended to remain in the brain longer after formulation (Fig. 5b and c). It is possible that nano-formulation is resistant to liver metabolism (Li and Huang, 2008) and so the concentration of curcumin in rat plasma decreased more slowly than conventional curcumin (plasma of Fig. 5). Consequently, the C-NPs in rat blood can be distributed to brain regions more constantly than conventional curcumin at 30 and 60 min time-points. Furthermore, a great deal of curcumin existed in the hippocampus for both curcumin and C-NPs group. It is noteworthy that curcumin accumulated more in the hippocampus than in other regions of the brain (Fig. 5), which may be because the transport of brain cells affects the disposition of compounds in different regions of the brain (Sarter and Parikh, 2005).

The pharmacokinetic parameters of curcumin in different brain regions after C-NPs and curcumin administration are shown in Table 3. The $t_{1/2}$ of curcumin in the cerebral cortex (from 2.32 to 19.9) and hippocampus (from 7.56 to 16.7) were significantly increased with curcumin encapsulated in nanoparticles. This $t_{1/2}$ increase was accompanied by a significant increase in MRT. As a result, the MRT values of the cerebral cortex and the hippocampus

Please cite this article in press as: Tsai, Y.-M., et al., Curcumin and its nano-formulation: The kinetics of tissue distribution and blood–brain barrier penetration. Int J Pharmaceut (2011), doi:10.1016/j.ijpharm.2011.06.030

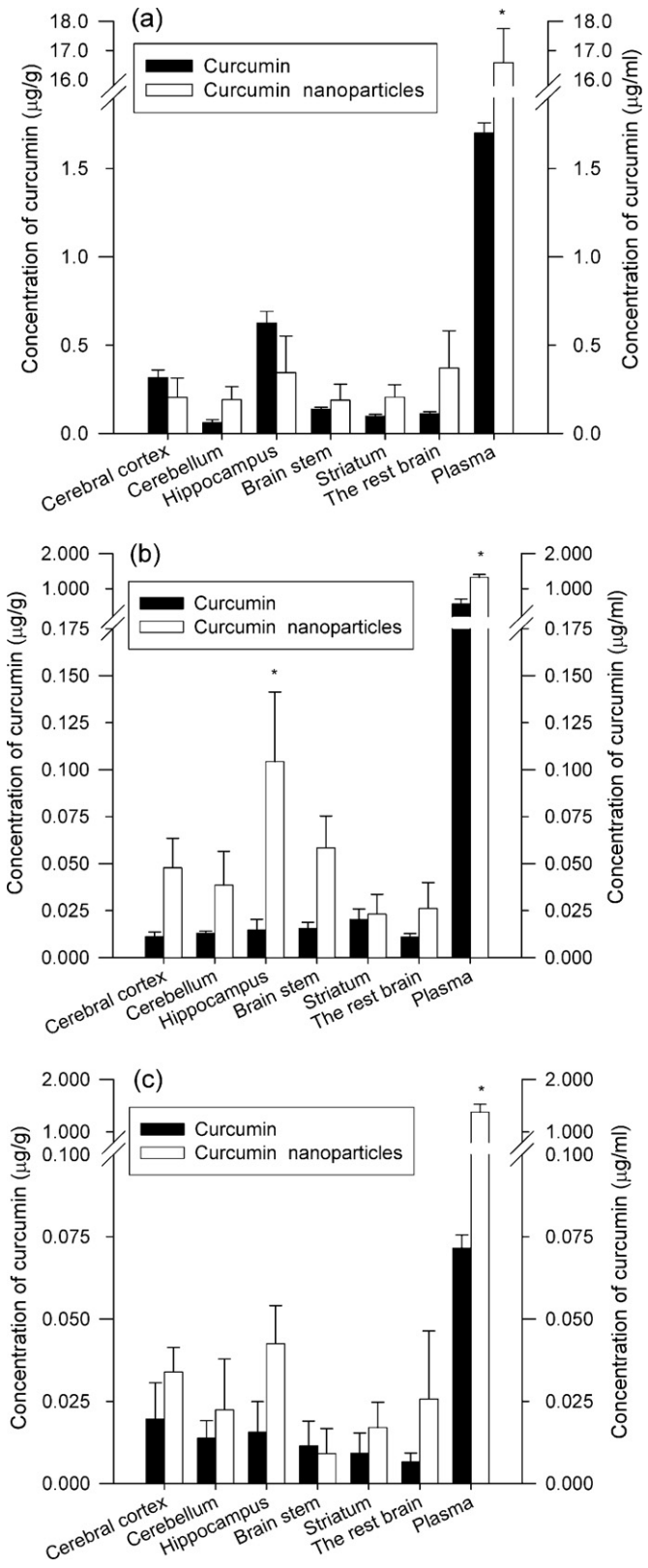

Fig. 5. Concentration of curcumin and C-NPs in different brain regions collected at (a) 15, (b) 30 and (c) 60 min after curcumin and C-NPs administration (i.v., 25 mg/kg, mean ± SEM, $n = 4$). ■: curcumin; □: C-NPs. *$p < 0.05$, vs. curcumin.

Table 3
Pharmacokinetic parameters of curcumin and C-NPs in different brain regions after i.v. administration.

Brain regions		$t_{1/2}$ (min)	AUC (min μg/ml)	MRT (min)
Cerebral cortex	C	2.32 ± 0.04	5.39 ± 0.78	17.9 ± 0.50
	C-NPs	19.9 ± 2.63*	6.55 ± 2.33	35.1 ± 4.50*
Cerebellum	C	16.9 ± 0.79	2.09 ± 0.24	31.5 ± 1.62
	C-NPs	17.9 ± 3.17	5.01 ± 2.24	30.6 ± 5.11
Hippocampus	C	7.56 ± 0.87	10.8 ± 1.42	16.5 ± 0.39
	C-NPs	16.7 ± 2.56*	11.7 ± 4.50	30.2 ± 4.25*
Brain stem	C	12.4 ± 0.79	2.49 ± 0.28	22.5 ± 1.10
	C-NPs	10.7 ± 1.55	3.96 ± 1.43	24.5 ± 2.09
Striatum	C	13.0 ± 1.98	1.74 ± 0.35	24.1 ± 1.35
	C-NPs	11.7 ± 0.66	3.01 ± 1.24	23.3 ± 1.06
The rest brain	C	12.1 ± 1.10	2.81 ± 0.89	21.9 ± 1.22
	C-NPs	11.0 ± 1.94	5.54 ± 3.57	22.4 ± 2.92

$t_{1/2}$: half-life; AUC: area under the concentration–time curve; MRT: mean residence time; C: curcumin; C-NPs: curcumin nanoparticles (mean ± SEM, $n = 4$).
* $p < 0.05$, vs. curcumin.

were increased about 2.0- and 1.8-fold, respectively. These results reveal that the retention time of curcumin in the cerebral cortex and the hippocampus was significantly increased by curcumin nano-formulation. Previous research has indicated that the cerebral cortex is a crucial region related to the development of epilepsy (Andrade, 2009). The hippocampus plays an important role in learning and memory, and its function is strongly related to patterns of dementia such as Alzheimer disease (Marlatt and Lucassen, 2010). However, Mancuso et al. (2011) have pointed out that the lack of therapeutic effect from conventional curcumin in the treatment of patients with Alzheimer disease could be attributable to the low concentration of curcumin in the brain. In addition, a recent study found that curcumin reduces the α-synuclein induced cytotoxicity of neurons (Wang et al., 2010) and another study shows that it protects mitochondria against peroxynitrite in nigrostriata, thereby slowing the progression of Parkinson's disease (Mythri et al., 2007). Although the concentration of curcumin in striatum was not significantly different between the two groups, the levels of curcumin after nano-formulation seemed to be higher than conventional curcumin. For these reasons, C-NPs might be more potent than conventional curcumin for treating certain brain diseases by maintaining the concentration level of curcumin in brain regions for longer periods of time.

According to these distribution results, curcumin can arrive in organs and regions of the brain, where it can perform its pharmacodynamic activities, as demonstrated by previous studies. After nano-formulation, the concentration and retention time of curcumin in these organs was significantly increased. These pharmacokinetic data suggest that C-NPs might offer greater therapeutic effect than conventional curcumin from a pharmacodynamic perspective. Therefore, the distribution results of curcumin and C-NPs to the site of action are vital for dose determination, time to administration and toxicity in pre-clinical and clinical therapeutic research.

4. Conclusion

In this study, an analytical method for determining curcumin and its nano-formulation in different organs was optimized. We demonstrated that curcumin and C-NPs were distributed to the liver, heart, spleen, lung, kidney and brain. Nano-formulation could significantly raise the AUC, $t_{1/2}$, and MRT of curcumin in all these organs, except the heart. Distribution levels in regions of the brain showed that curcumin accumulated in the hippocampus for both formulations of curcumin. The retention times of curcumin in the cerebral cortex and hippocampus were significantly extended by

Please cite this article in press as: Tsai, Y.-M., et al., Curcumin and its nano-formulation: The kinetics of tissue distribution and blood–brain barrier penetration. Int J Pharmaceut (2011), doi:10.1016/j.ijpharm.2011.06.030

PLGA nanoparticle encapsulation. These results provide information to help more effectively in employing curcumin and to clarify its formulation in therapeutic applications.

Acknowledgements

Funding for this study was provided in part by research Grants: NSC99-2113-M-010 -001-MY3 and NSC99-2628-B-010-008-MY3 from the National Science Council, Taiwan; TCH 99001-62-007 from Taipei City Hospital, 99-EC-17-A-17-S1-152 from Technology Development Program for Academia, Ministry of Economic Affairs, Taiwan.

References

Abdelwahed, W., Degobert, G., Stainmesse, S., Fessi, H., 2006. Freeze-drying of nanoparticles: formulation, process and storage considerations. Adv. Drug. Deliv. Rev. 58, 1688–1713.
Alam, M.I., Beg, S., Samad, A., Baboota, S., Kohli, K., Ali, J., Ahuja, A., Akbar, M., 2010. Strategy for effective brain drug delivery. Eur. J. Pharm. Sci. 40, 385–403.
Ammon, H., Wahl, M.A., 1991. Pharmacology of *Curcuma longa*. Planta Med. 57, 1–7.
Anand, P., Kunnumakkara, A.B., Newman, R.A., Aggarwal, B.B., 2007. Bioavailability of curcumin: problems and promises. Mol. Pharm. 4, 807–818.
Anand, P., Nair, H.B., Sung, B., Kunnumakkara, A.B., Yadav, V.R., Tekmal, R.R., Aggarwal, B.B., 2010. Design of curcumin-loaded PLGA nanoparticles formulation with enhanced cellular uptake, and increased bioactivity in vitro and superior bioavailability in vivo. Biochem. Pharmacol. 79, 330–338.
Andrade, D.M., 2009. Genetic basis in epilepsies caused by malformations of cortical development and in those with structurally normal brain. Hum. Genet. 126, 173–193.
Chien, C.F., Wu, Y.T., Lee, W.C., Lin, L.C., Tsai, T.H., 2010. Herb–drug interaction of Andrographis paniculata extract and andrographolide on the pharmacokinetics of theophylline in rats. Chem. Biol. Interact. 184, 458–465.
DeMerlis, C.C., Schoneker, D.R., 2003. Review of the oral toxicity of polyvinyl alcohol (PVA). Food Chem. Toxicol. 41, 319–326.
Faisant, N., Siepmann, J., Benoit, J.P., 2002. PLGA-based microparticles: elucidation of mechanisms and a new, simple mathematical model quantifying drug release. Eur. J. Pharm. Sci. 15, 355–366.
Garcia-Alloza, M., Borrelli, L.A., Rozkalne, A., Hyman, B.T., Bacskai, B.J., 2007. Curcumin labels amyloid pathology in vivo, disrupts existing plaques, and partially restores distorted neurites in an Alzheimer mouse model. J. Neurochem. 102, 1095–1104.
Gururajan, M., Dasu, T., Shahidain, S., Jennings, C.D., Robertson, D.A., Rangnekar, V.M., Bondada, S., 2007. Spleen tyrosine kinase (Syk), a novel target of curcumin, is required for B lymphoma growth. J. Immunol. 178, 111–121.
He, C., Hu, Y., Yin, L., Tang, C., Yin, C., 2010. Effects of particle size and surface charge on cellular uptake and biodistribution of polymeric nanoparticles. Biomaterials 31, 3657–3666.
Higuchi, T., 1963. Mechanism of sustained-action medication. Theoretical analysis of rate of release of solid drugs dispersed in solid matrices. J. Pharm. Sci. 52, 1145–1149.
Jaiswal, J., Gupta, S.K., Kreuter, J., 2004. Preparation of biodegradable cyclosporine nanoparticles by high-pressure emulsification-solvent evaporation process. J. Control. Release 96, 169–178.
Kim, T.H., Jiang, H.H., Youn, Y.S., Park, C.W., Tak, K.K., Lee, S., Kim, H., Jon, S., Chen, X., Lee, K.C., 2011. Preparation and characterization of water-soluble albumin-bound curcumin nanoparticles with improved antitumor activity. Int. J. Pharm. 403, 285–291.
Lankveld, D.P., Oomen, A.G., Krystek, P., Neigh, A., Troost-de Jong, A., Noorlander, C.W., Van Eijkeren, J.C., Geertsma, R.E., De Jong, W.H., 2010. The kinetics of the tissue distribution of silver nanoparticles of different sizes. Biomaterials, PMID: 20684985.
Li, S.D., Huang, L., 2008. Pharmacokinetics and biodistribution of nanoparticles. Mol. Pharm. 5, 496–504.
Liang, H.F., Yang, T.F., Huang, C.T., Chen, M.C., Sung, H.W., 2005. Preparation of nanoparticles composed of poly(gamma-glutamic acid)-poly(lactide) block copolymers and evaluation of their uptake by HepG2 cells. J. Control. Release 105, 213–225.
Ma, Z., Shayeganpour, A., Brocks, D.R., Lavasanifar, A., Samuel, J., 2007. High-performance liquid chromatography analysis of curcumin in rat plasma: application to pharmacokinetics of polymeric micellar formulation of curcumin. Biomed. Chromatogr. 21, 546–552.
Mancuso, C., Siciliano, R., Barone, E., 2011. Curcumin and Alzheimer disease: this marriage is not to be performed. J. Biol. Chem. 285, 28472–28480.
Manikandan, R., Thiagarajan, R., Beulaja, S., Sudhandiran, G., Arumugam, M., 2010. Curcumin protects against hepatic and renal injuries mediated by inducible nitric oxide synthase during selenium-induced toxicity in Wistar rats. Microsc. Res. Tech. 73, 631–637.
Marlatt, M.W., Lucassen, P.J., 2010. Neurogenesis and Alzheimer's disease: biology and pathophysiology in mice and men. Curr. Alzheimer Res. 7, 113–125.
Mastrobattista, E., Koning, G.A., Storm, G., 1999. Immunoliposomes for the targeted delivery of antitumor drugs. Adv. Drug Deliv. Rev. 40, 103–127.
Moghaddam, S.J., Barta, P., Mirabolfathinejad, S.G., Ammar-Aouchiche, Z., Garza, N.T., Vo, T.T., Newman, R.A., Aggarwal, B.B., Evans, C.M., Tuvim, M.J., Lotan, R., Dickey, B.F., 2009. Curcumin inhibits COPD-like airway inflammation and lung cancer progression in mice. Carcinogenesis 30, 1949–1956.
Moghimi, S.M., Hunter, A.C., Murray, J.C., 2001. Long-circulating and target-specific nanoparticles: theory to practice. Pharmacol. Rev. 53, 283–318.
Mohanty, C., Sahoo, S.K., 2010. The in vitro stability and in vivo pharmacokinetics of curcumin prepared as an aqueous nanoparticulate formulation. Biomaterials 31, 6597–6611.
Müller, R.H., 1991. Colloidal Carriers for Controlled Drug Delivery and Targeting. CRC Press, Boca Raton, pp. 45–56.
Mythri, R.B., Jagatha, B., Pradhan, N., Andersen, J., Bharath, M.M., 2007. Mitochondrial complex I inhibition in Parkinson's disease: how can curcumin protect mitochondria? Antioxid. Redox. Signal. 9, 399–408.
Park, T.G., 1995. Degradation of poly(lactic-*co*-glycolic acid) microspheres: effect of copolymer composition. Biomaterials 16, 1123–1130.
Purkayastha, S., Berliner, A., Fernando, S.S., Ranasinghe, B., Ray, I., Tariq, H., Banerjee, P., 2009. Curcumin blocks brain tumor formation. Brain Res. 1266, 130–138.
Sarter, M., Parikh, V., 2005. Choline transporters, cholinergic transmission and cognition. Nat. Rev. Neurosci. 6, 48–56.
Schmidt, S., Gonzalez, D., Derendorf, H., 2010. Significance of protein binding in pharmacokinetics and pharmacodynamics. J. Pharm. Sci. 99, 1107–1122.
Sethi, P., Jyoti, A., Hussain, E., Sharma, D., 2009. Curcumin attenuates aluminium-induced functional neurotoxicity in rats. Pharmacol. Biochem. Behav. 93, 31–39.
Shaikh, J., Ankola, D.D., Beniwal, V., Singh, D., Kumar, M.N., 2009. Nanoparticle encapsulation improves oral bioavailability of curcumin by at least 9-fold when compared to curcumin administered with piperine as absorption enhancer. Eur. J. Pharm. Sci. 37, 223–230.
Shehzad, A., Wahid, F., Lee, Y.S., 2010. Curcumin in cancer chemoprevention: molecular targets, pharmacokinetics, bioavailability, and clinical trials. Arch. Pharm. 343, 489–499.
Sumanont, Y., Murakami, Y., Tohda, M., Vajragupta, O., Watanabe, H., Matsumoto, K., 2007. Effects of manganese complexes of curcumin and diacetylcurcumin on kainic acid-induced neurotoxic responses in the rat hippocampus. Biol. Pharm. Bull. 30, 1732–1739.
Tsai, Y.M., Jan, W.C., Chien, C.F., Lee, W.C., Lin, L.C., Tsai, T.H., 2011. Optimised nano-formulation on the bioavailability of hydrophobic polyphenol, curcumin, in freely-moving rats. Food Chem., doi:10.1016/j.foodchem.2011.01.059.
Wang, M.S., Boddapati, S., Emadi, S., Sierks, M.R., 2010. Curcumin reduces alpha-synuclein induced cytotoxicity in Parkinson's disease cell model. BMC Neurosci. 11, 57–67.
Wu, S.J., Tam, K.W., Tsai, Y.H., Chang, C.C., Chao, J.C., 2010. Curcumin and saikosaponin an inhibit chemical-induced liver inflammation and fibrosis in rats. Am. J. Chin. Med. 38, 99–111.
Yallapu, M.M., Gupta, B.K., Jaggi, M., Chauhan, S.C., 2010. Fabrication of curcumin encapsulated PLGA nanoparticles for improved therapeutic effects in metastatic cancer cells. J. Colloid Interface Sci., PMID: 20627257.
Yang, K.Y., Lin, L.C., Tseng, T.Y., Wang, S.C., Tsai, T.H., 2007. Oral bioavailability of curcumin in rat and the herbal analysis from *Curcuma longa* by LC-MS/MS. J. Chromatogr. B: Analyt. Technol. Biomed. Life Sci. 853, 183–189.
Zolnik, B.S., Burgess, D.J., 2007. Effect of acidic pH on PLGA microsphere degradation and release. J. Control. Release 122, 338–434.
Zolnik, B.S., Leary, P.E., Burgess, D.J., 2006. Elevated temperature accelerated release testing of PLGA microspheres. J. Control. Release 112, 293–300.

Please cite this article in press as: Tsai, Y.-M., et al., Curcumin and its nano-formulation: The kinetics of tissue distribution and blood–brain barrier penetration. Int J Pharmaceut (2011), doi:10.1016/j.ijpharm.2011.06.030